Translational Oncology 56 (2025) 102401

Contents lists available at ScienceDirect

Translational Oncology

journal homepage: www.elsevier.com/locate/tranon

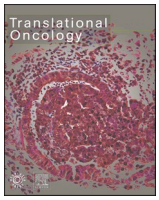

miR-4537 curtails ferroptosis by targeting MIOX in renal cell carcinoma

Hui Li [a,b,*], Mengyu Fu [a,b], Lingli Wang [a,b], Yanpeng Dai [a,b], Zongxing Lv [a,b], Shilin Geng [a,b]

[a] Department of Laboratory Medicine, the Third Affiliated Hospital of Zhengzhou University, Zhengzhou, Henan, China
[b] Zhengzhou Key Laboratory for In Vitro Diagnosis of Hypertensive Disorders of Pregnancy, Zhengzhou, Henan, China

ARTICLE INFO

Keywords:
Mir-4537
MIOX
Ferroptosis
ccRCC
Cancer therapy

ABSTRACT

Ferroptosis, an iron-dependent mode of cell death, has gained prominence for its critical role in the advancement of various cancers, notably clear cell renal carcinoma (ccRCC). The intricacies of ferroptosis's involvement in ccRCC, however, remain largely undefined. This study aimed to dissect the contribution of ferroptosis to ccRCC by examining differentially expressed genes (DEGs) identified within the TCGA ccRCC database and ferroptosis driver genes catalogued in the FerrDb database (dedicates to ferroptosis regulators and ferroptosis-disease associations). We employed 786-O and ACHN ccRCC cell lines, alongside HK2 (human kidey-2) cells and HKC (human kidney cells), to confirm the expression of 9 shared genes. Among these, MIOX (myo-inositol oxygenase) emerged as significantly downregulated in ccRCC cells compared to HK2 and HKC cells. Subsequent survival analysis illuminated a positive correlation between MIOX expression and improved patient survival, underscoring its prognostic significance. Further investigations into MIOX regulation identified four miRNAs via TargetScan predictions, with miR-4537 significantly upregulated in ccRCC cell lines. Functional assays involving miR-4537 mimics and inhibitors, combined with ferroptosis inducers and inhibitors, elucidated its impact on ccRCC cell growth and ferroptosis modulation. The results revealed that miR-4537 expression was diminished following ferroptosis induction, and the miR-4537 inhibitor markedly curbing ccRCC cell proliferation by fostering ferroptosis, while the mimic exerted opposite effects. Mechanistically, miR-4537 targets the 3′-UTR of MIOX to manipulate its expression, ultimately inhibiting ferroptosis in ccRCC cells. Our research indicated that miR-4537 restrained ferroptosis by regulating MIOX in ccRCC, offering novel insights into the mechanisms of ferroptosis in cancer biology and highlighting latent therapeutic avenues for cancer treatment through ferroptosis modulation.

Introduction

Renal cell carcinomas (RCCs) account for over 90 % of all kidney cancers and originate from the kidney epithelium. These carcinomas are characterized by their notable heterogeneity, encompassing more than ten distinct histologic and molecular subtypes [1]. Among these, clear cell RCC (ccRCC) is the most common subtype and the primary contributor to kidney cancer-related mortality [2]. Although ccRCC is a disorder that could be considered curable with successful surgery or ablative strategies, metastasis occurs in up to one-third of cases [3]. Such a disease state is invariably lethal and exhibits a critical distinction when we consider the biology of ccRCC [4]. Furthermore, despite substantial progress in immunotherapy and molecular targeted therapy for ccRCC, treatment outcomes have not been satisfactory [5]. Therefore, it is particularly important to elucidate the pathogenesis of ccRCC and investigate alternative approaches to treat ccRCC.

Contemporary cancer therapies aim to selectively target cancer cells while sparing non-malignant cells, with the induction of apoptosis by anti-cancer drugs being a primary mechanism for eliminating tumor cells [6]. However, due to defects in apoptotic pathways, cancer cells often exhibit resistance to apoptosis, limiting the efficacy of such treatments. Cancer cells, to support their rapid proliferation, require more iron than healthy cells, making them more susceptible to iron-catalyzed necrosis, or ferroptosis [7]. Ferroptosis, an iron-dependent form of regulated cell death, has emerged as a significant player in cancer biology tumors [8,9]. This process is characterized by the accumulation of lipid peroxides to lethal levels, leading to cell death distinct from apoptosis and necrosis. Iron serves as a catalyst in this process; its accumulation can initiate the Fenton reaction, producing reactive oxygen species that promote lipid peroxidation [10]. Recent

* Corresponding author.
E-mail address: lihuilizi120@163.com (H. Li).

https://doi.org/10.1016/j.tranon.2025.102401
Received 3 March 2025; Received in revised form 5 April 2025; Accepted 19 April 2025

studies have revealed that ferroptosis serves as dual-effector in cancers. Interestingly, ferroptosis has been confirmed to repress cancer progression by impairing the malignant phenotype of cancer cells ranging from blood tumors to multiple solid tumors [11]. Notably, studies have shown that inactivation of glutathione peroxidase 4 (GPX4), an enzyme that detoxifies lipid peroxides, leads to ferroptosis and inhibits tumor growth. Conversely, ferroptosis has also been implicated in promoting metastasis and resistance to therapy in some cancer contexts [12]. Cancer cells, particularly those resistant to traditional therapies, often exhibit increased sensitivity to ferroptosis, making it a potential target for novel cancer treatments [10]. From a mechanistic standpoint, the impairment of the cell membrane occurs due to the iron-catalyzed buildup of robust membrane lipid peroxidation (LPO) and the subsequent initiation of oxidative stress [13]. Targeting ferroptosis has triggered substantial interest from the oncology community as it may provide novel avenues for anticancer treatment that are refractory to conventional therapies.

MicroRNAs (miRNAs), the diminutive architects of the cellular world, encompass 20–22 nucleotides and orchestrate gene expression with precision. They wield their influence by latching onto complementary sequences within mRNAs, a process that typically culminates in the strategic silencing of gene activity post-transcription [14]. Mounting studies disclosed that numerous miRNAs possess the dual capacity to function as either oncogenes or tumor suppressors, playing a critical role in the pathogenesis and advancement of ccRCC [15]. Despite extensive research efforts to elucidate the role of miRNAs in ccRCC, current understanding represents just the beginning, with the functions of many miRNAs still largely unexplored.

This investigation sought to clarify the potential role of ferroptosis in ccRCC by examining critical differentially expressed genes and ferroptosis-inducing genes in the Ferrdb database (dedicates to ferroptosis regulators and ferroptosis-disease associations). To explore the potential role of ferroptosis in ccRCC, we performed a systematic screening of relevant genes associated with ferroptosis. We first obtained RNA sequencing data for ccRCC from TCGA-KIRC (kidney renal clear cell carcinoma) project, which provides comprehensive genomic information for ccRCC. Using differential expression analysis through the DESeq2, we identified genes that were significantly downregulated in ccRCC. These differentially expressed genes (DEGs) were then cross-referenced with ferroptosis driver genes cataloged in the Ferrdb database (http://www.zhounan.org/ferrdb/), which compiles known ferroptosis-related genes, including drivers, suppressors, and markers. By intersecting the DEGs from the TCGA ccRCC dataset with the ferroptosis-related genes from Ferrdb, we were able to pinpoint a list of genes that may play critical roles in ferroptosis regulation in the context of ccRCC. By integrating these datasets, we aimed to identify key genes that may play critical roles in ferroptosis regulation in ccRCC. The study's objectives include examining the association between ferroptosis-related genes and ccRCC progression, understanding how these genes influence tumor growth, and investigating potential molecular mechanisms involved. Furthermore, we sought to explore the regulatory role of miR-4537 in modulating ferroptosis through the regulation of key genes like MIOX (myo-inositol oxygenase). We expect that our findings will contribute to a deeper understanding of ferroptosis in ccRCC, providing novel insights into its mechanistic pathways and identifying potential therapeutic targets for intervention in ccRCC treatment. By elucidating the regulatory network involving miR-4537 and MIOX, this study has the potential to open new avenues for targeted therapies aimed at inducing ferroptosis in ccRCC cells.

Material and methods

Collection of data

To elucidate the involvement of ferroptosis in ccRCC, we leveraged the *Ferrdb* gene database (http://www.zhounan.org/ferrdb/), to identify associated genes. Further, RNA sequencing data specific to ccRCC was procured from the TCGA-KIRC project (https://portal.gdc.cancer.gov/). For RNA-seq data analysis, the FPKM data was converted to TPM format and subsequently transformed to log2 scale. Differential expression analysis was conducted exploiting the DESeq2 package in R [16], with significant genes identified based on an adjusted p-value less than 0.05 combined with an absolute fold change exceeding 2.

Table 1
Primer sequences of the relevant mRNAs and miRNAs.

Genes	Forward primer (5′–3′)	Reverse primer (5′–3′)
GAPDH	GGAGCGAGATCCCTCCAAAAT	GGCTGTTGTCATACTTCTCATGG
AQP3	CCGTGACCTTTGCCATGTG	CGAAGTGCCAGATTGCATCATAA
ACADSB	TCTTGGGACAAATTGGACATGG	GTGAGCCACTTGGTGTTGGA
ACSF2	GCCTCAGCTACGTTCAGGG	CATAGGAGTTAGGTCCCCACA
MIOX	CTGGTGGATGAGTCGGACC	GAGTCGCAGAAAACCACGG
AQP5	CGGGCTTTCTTCTACGTGG	GCTGGAAGGTCAGAATCAGCTC
IFNA14	TGGGCTGTAATCTGTCTCAAAC	TAGGAGGGTCTCATCCCAAGC
IFNA7	AGGGCCTTGATACTCCTGG	TCCTCCTCCGGGAATCTGAAT
TTPA	ACTCAGCGGAATGGAATCAAG	TGCCACGAACTTTCAATGGAA
DPEP1	CAAGTGGCCGACCATCTGG	GGGACCCTTGGAACACCATC
miR-4537	TGAGCCGAGCTGAGCTT	CAGTGCGTGTCGTGGAGT
miR-4635	GGACCTCTTGAAGTCAGAACC	CAGTGCGTGTCGTGGAGT
miR-4538	GGACCAGCTTGGATGAGCTGG	CAGTGCGTGTCGTGGAGT
miR-8083	GGCAGGACTTGACGGCTG	CAGTGCGTGTCGTGGAGT
U6	CTCGCTTCGGCAGCACA	AACGCTTCACGAATTTGCGT

Treatment and culture of cells

Cell lines specific to ccRCC—ACHN and 786-O—as well as HK2 (human kidney −2) cells and HKC (human kidney cell, proximal tubule cell) were acquired from the National Collection of Authenticated Cell Cultures Center and the American Type Culture Collection. The maintenance of these cell cultures was conducted in DMEM sourced from Hyclone, USA, supplemented with 10 % FBS and 1 % penicillin-streptomycin (Sigma, USA). Cultivation took place under precise conditions: a temperature of 37 °C and an atmosphere composed of 95 % humidity and 5 % CO_2. GenePharm Ltd (Shanghai, China) synthesized the miR-4537 mimic and inhibitor, alongside their respective controls, to modulate miR-4537 expression in ccRCC cells via transfection. Transfection was carried out using Lipofectamine 3000 reagent upon cells reaching 70–80 % confluency, adhering to the manufacturer's protocol with slight modifications. To induce ferroptosis, Erastin and RSL3 were introduced to the cell culture, with DMSO serving as the negative control [17]. Pre-treatment involved transfecting ccRcc cell lines with the miR-4537 mimic or inhibitor for 24–48 h, followed by exposure to 0.2 μmol/L liproxstatin-1 for an additional 48–72 h, to evaluate ferroptosis induction.

Expression detection of MIOX in ccRCC

We introduced qRT-PCR analysis to explore the association between miR-4753 and MIOX in ccRCC. The concentration and quality of isolated RNA from 786-O, ACHN, HK2, and HKC cells were evaluated by NanoDrop 2000 using Trizol reagent. For mRNA analysis, 1 μg of RNA was reverse-transcribed into cDNA employing the AceQ Universal SYBR qPCR Master Mix provided by Vazyme, China. Similarly, for miRNA quantification, 1 μg of RNA underwent cDNA synthesis utilizing the miRNA 1st Strand cDNA Synthesis Kit (Vazyme, China). The expression levels of mRNA and miRNA across various samples were quantitatively assessed via real-time PCR($2^{-\Delta\Delta ct}$), exploiting the AceQ qPCR SYBR Green Master Mix [18]. miRNA level was normalized to U6 expression and mRNA expression was normalized to GAPDH expression. The primers sequence were listed as Table 1.

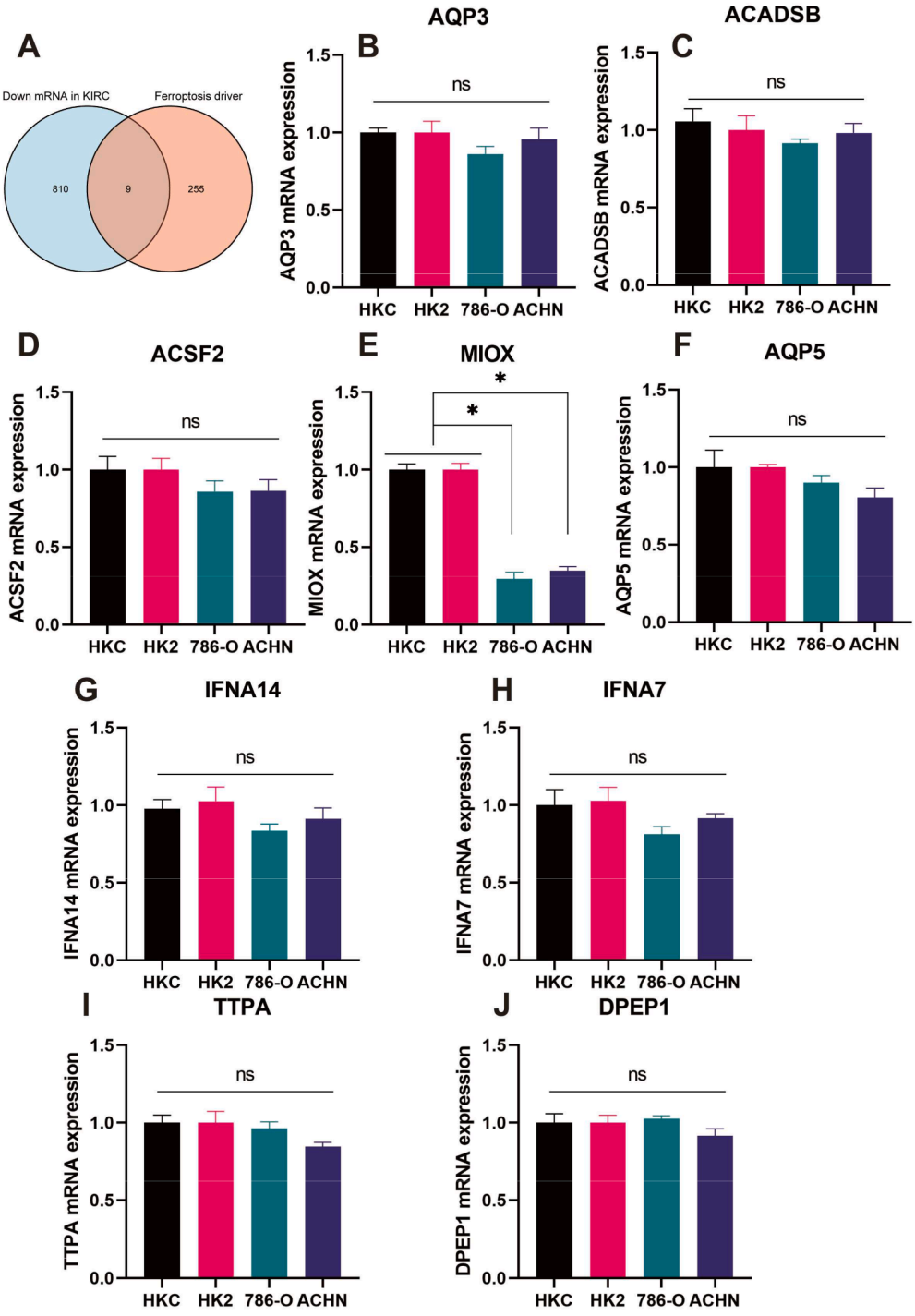

Fig. 1. MIOX expression was significantly decreased in ccRCC cells. (A) The Venn results of down-regulated mRNAs in ccRCC and ferroptosis driver geneset. (B-J) The expression of 9 common genes including *AQP3, ACADSB, ACSF2, MIOX, AQP5, IFNA7, IFNA14, TTPA,* and *DEEP1* in ccRCC and proximal tubule cell lines. (ns, not significant; $^*P < 0.05$).

The miR-4537 dysfunction influenced cell viability in ccRCC

Cell viability was used to explore the influence of miR-4537 on ccRCC growth. We used CCK-8 assay to investigate the cell survival rate when treated with miR-4537 mimic or inhibitor. Briefly speaking, cells, both treated and untreated, were evenly distributed across a 96-well plate at uniform densities [19]. Then 10μl working solution was combined with the cell supernatants for 2 h under a dark environment. The absorbance of the medium at 450 nm was tested to determine cell viability. In contrast, the lactate dehydrogenase (LDH) concentration in cell supernatants was analyzed to determine cell mortality using an LDH Cytotoxicity Detection Kit (Takara) as suggested by the manufacturer and a previous study [20]. Cell supernatants were combined with an equal volume of LDH working reagent and incubated for 30 min in a dark environment before validating the absorbance at 500 nm with a spectrophotometer.

Colony formation assay to assess ccrcc cell proliferation

We introduced the colony formation assay to evaluate the growth

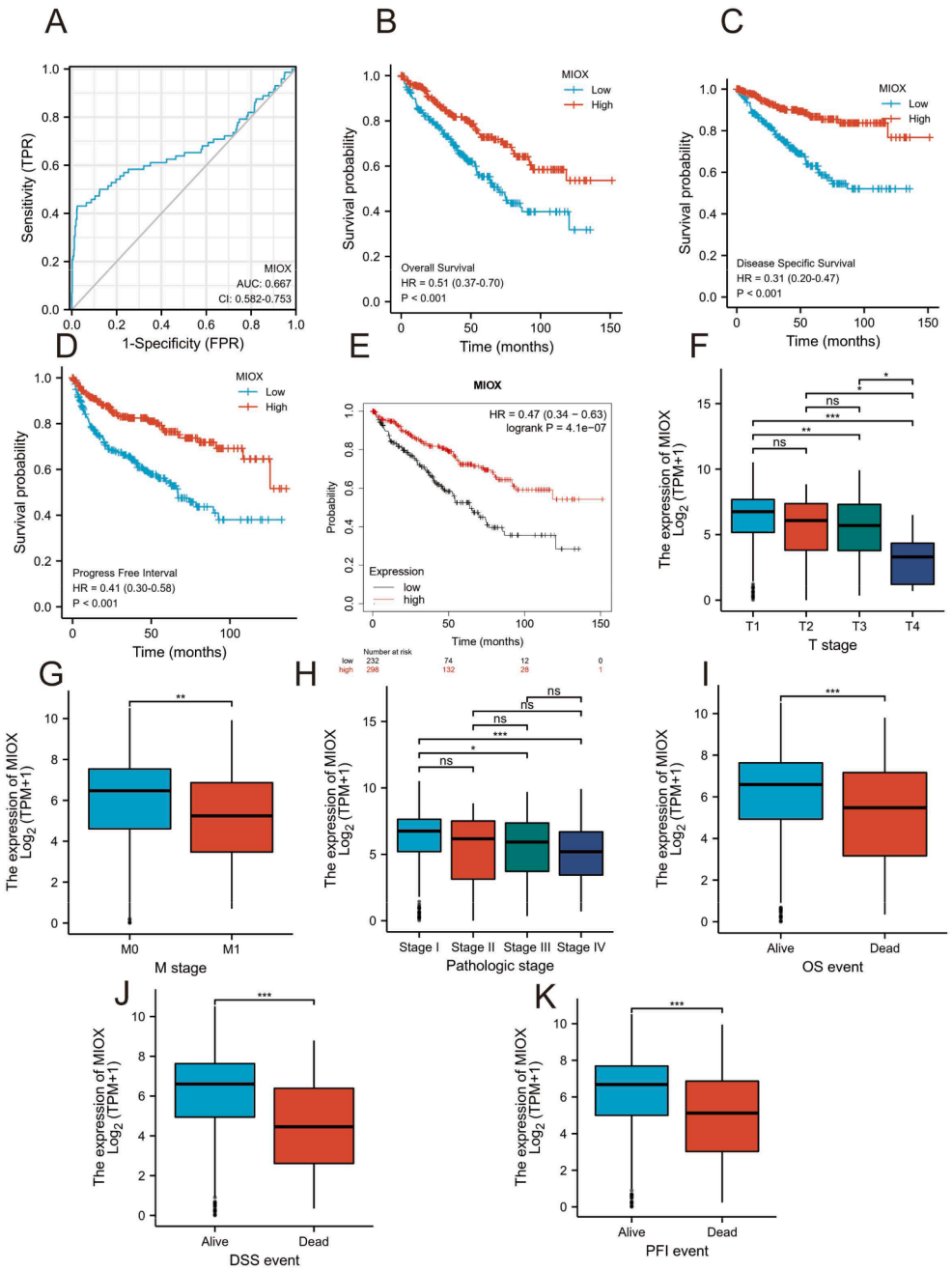

Fig. 2. The survival analysis of *MIOX* in ccRCC. (A) The ROC result of *MIOX* in ccRCC. (B-D) Overall survival, disease-specific survival, and progress-free analysis of *MIOX* in TCGA ccRCC. (E) The overall survival analysis of *MIOX* in ccRCC was based on the KM plotter database. (F-H) The expression of *MIOX* in different T, M, and pathological stages of ccRCC in TCGA. (I-K) The expression landscape of *MIOX* in OS, DSS, and PFS survivor groups and non-survivor groups. (ns, not significant; $^{*}P < 0.05$, $^{**}P < 0.01$, $^{***}P < 0.001$).

ability of ccRCC in vitro [21]. In summary, ccRCC cells were cultured for 2 weeks, either treated with miR-4537 mimic, miR-4537 inhibitor, or left untreated. Following this, cell duplicates were treated with methanol for a duration of 30 min, then stained with crystal violet for 15–20 min after discarding the liquid above them. Finally, the staining solution was cleared up by PBS three times for the image analysis. Cell counts were calculated by Image J software.

Intracellular ROS measurement to evaluate oxidative stress in ccrcc cells

This assay was performed to assess oxidative stress-induced membrane damage, a hallmark of ferroptosis, by measuring the intracellular reactive oxygen species (ROS) levels in ccRCC cells. We measured intracellular ROS levels using a LPO assay kit provided by Jiancheng Bioengineering Institute. The procedure involved treating cell cultures with DCFH-DA dye for 30 min at 37 °C. Fluorescence intensity was measured at 488/525 nm excitation/emission wavelengths to quantify intracellular ROS activity.

Lipid peroxidation (LPO) and antioxidant status assessment in ccrcc cells

This experiment aimed to measure lipid peroxidation (LPO) and evaluate the oxidative stress response associated with ferroptosis in ccRCC cells. We assessed LPO in ACHN and 786-O cells using an LPO assay kit from Jiancheng Bioengineering Institute. Absorbance at 586 nm was measured using a Thermo spectrophotometer to determine the

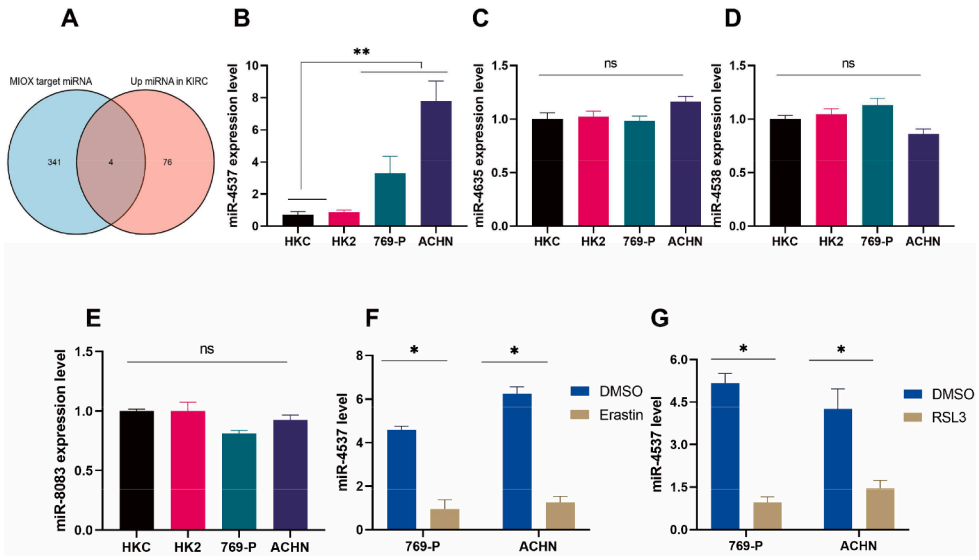

Fig. 3. miR-4537 was up-regulated in ccRCC via qRT-PCR. (A) The Venn result of *MIOX* target miRNA and up-regulated mRNA in TCGA ccRCC cohort. (B-E) The expression of miR-4537, miR-4635, miR-4638, and miR-8083 in ccRCC and proximal tubule cell lines. (F-G) miR-4537 expression level after ccRCC cells treated with ferroptosis inducer Erastin or RSL3. (ns, not significant; $^{*}P < 0.05$, $^{**}P < 0.01$).

concentration of LPO in the cell media after incubation with the assay reagents. Additionally, levels of 5-HETE, 12-HETE, and 15-HETE were quantified employing commercially available ELISA kits. The indicators of ferroptosis fighting systems such as GPX4 and GSH were also tested as previously reported [22]. Cells underwent lysis and were then subjected to deproteinization with PCA solution. The supernatant, obtained after centrifugation at 12,000 rpm and 4 °C for 15 min, was incubated with GST reagent and MCB for 30 min. Fluorescence was examined employing a SpectraMax plate reader at 380/460 nm excitation/emission wavelengths for GSH detection, which utilized phosphatidylcholine hydroperoxide as a substrate.

ATP quantification to assess cellular viability and energy status in ccrcc cells

The ATP detection assay was used to measure the cellular energy status as an indicator of cellular viability and function under ferroptosis-inducing conditions. For ATP measurement, the Cell Counting Kit-Luminescence kit (DOJINDO) was used to test ATP in cells by luciferase [23]. Briefly, the same volume of ATP working solution was added into cell supernatants after overnight culture. After incubation for 10 min undergoing concussion, the luminescence value was detected.

Iron quantification to investigate ferroptosis in ccrcc cells

This assay was used to quantify the intracellular iron content, which is essential for the induction of ferroptosis. Iron metabolism is fundamental to the induction of ferroptosis. To quantify the intracellular iron content, we utilized an iron colorimetric assay kit from Abcam, following the manufacturer's instructions [24]. This assay facilitated the measurement of intracellular iron levels by determining the absorbance of the assay mixture at 590 nm.

Luciferase reporter assay to investigate regulation of miR-4537 in MIOX expression

The luciferase reporter assay was conducted to assess the direct interaction between miR-4537 and the 3′-UTR of *MIOX* according to a previous study [25]. The wild-type and truncated 3′-UTR sequences of *MIOX* were cloned into the original pGL3-Basic plasmid (GenScript, China). The resultant cloned plasmids were then transfected into HEK293T cells in conjunction with a miR-4537 mimic by Lipofectamine 3000 reagent (Thermo Fisher Scientific Inc, USA). After a 48-hour incubation period, luciferase performance in the co-transfected cells from different experimental groups was quantitatively assessed by adopting a dual luciferase reporter assay system.

Statistical analysis

Statistical evaluations were carried out utilizing GraphPad Prism, with data representation grounded in means and standard deviations. Analysis of variance (ANOVA) served as the primary method for discerning significant disparities among groups, thereby enabling comprehensive comparisons across diverse experimental scenarios. Subsequently, Bonferroni was conducted to identify specific group comparisons that were significant. Kaplan-Meier survival curves, analyzed with the log-rank test, were used to evaluate treatment efficacy. A threshold p-value of less than 0.05 was established as the criterion for statistical significance.

Results

qRT-PCR analysis showed MIOX is down-regulated in ccRCC

In order to categorize the connection within ferroptosis and ccRCC, we obtained the ferroptosis driver genes from a database dedicated to ferroptosis, totaling 264 genes recognized as ferroptosis driver genes. Also, we obtained the down-regulated mRNAs in ccRCC from the TCGA database. With the screening criteria fold change ≤ -2, a total of 819 features were figured out for subsequent investigation. We acquired nine common genes from the previous two gene lists (Fig. 1A). These gene lists have been placed in Supplementary File 1. Afterward, we examined the expression profiles in ccRCC cell lines (786-O and ACHN) as well as human proximal tubule cell lines (HKC and HK-2). Result showed *MIOX* was significantly downregulated in ccRCC cell lines ($P < 0.05$) while other genes such as *AQP3, AQP5*, and *ACSF2* showed insignificant expression in ccRCC cell lines compared to proximal tubule cell lines (Fig. 1B-H). Therefore, we focused on the *MIOX* in the following research. These investigations demonstrated that *MIOX* expression was significantly decreased in ccRCC and involved with ccRCC progression.

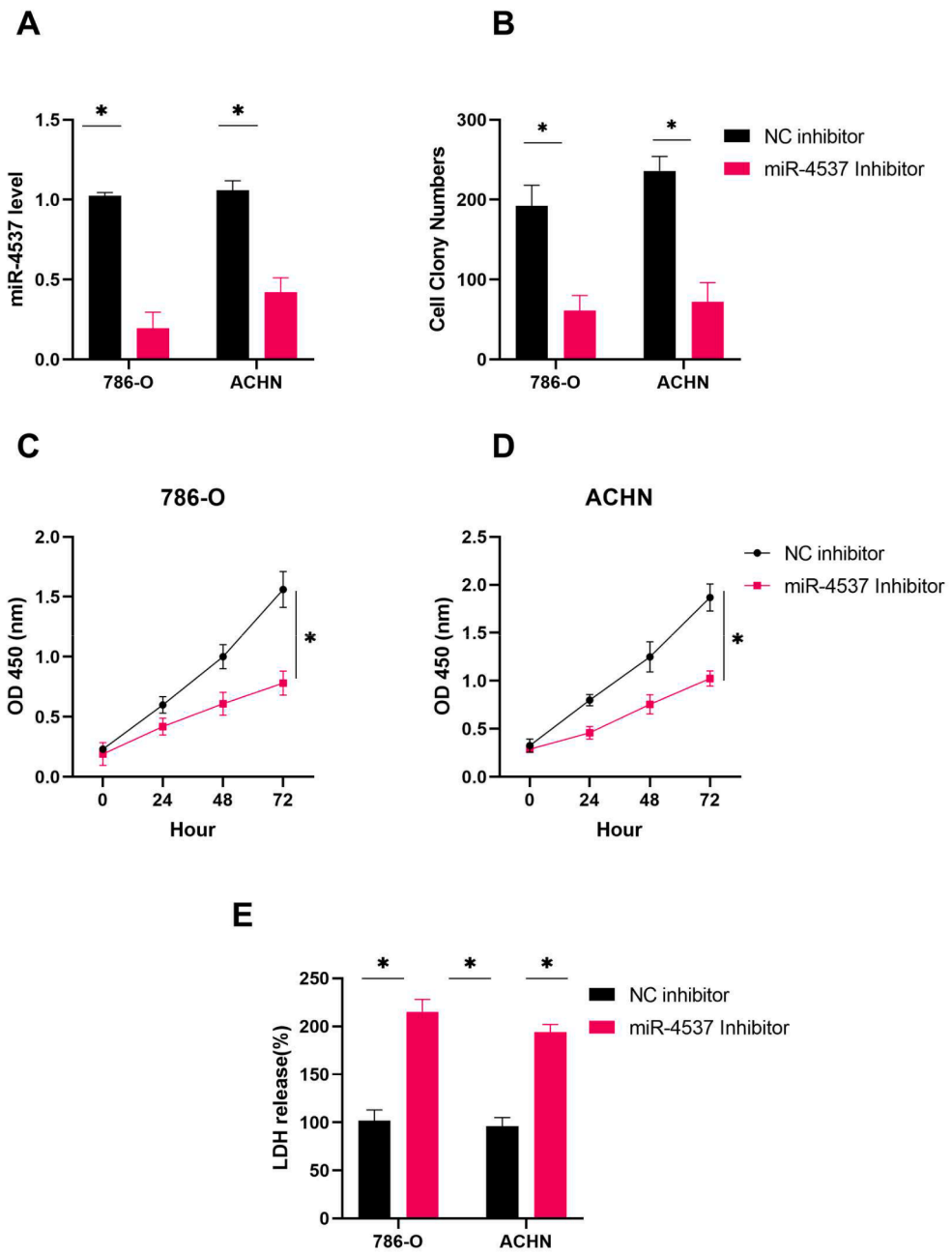

Fig. 4. miR-4537 inhibitor curbed ccRCC cell proliferation. (A)The miR-4537 inhibitor reduced miR-4537 expression in both 786-O and ACHN cells. (B) The number of colony-forming cells decreased after the cells were transfected with the miR-4537 inhibitor. (C-D) CCK-8 results of 786-O and ACHN cells treated with miR-4537 inhibitor. (E) The LDH generation volume of cells stimulated with miR-4537 inhibitor. (ns, not significant; *$P < 0.05$).

MIOX is associated with ccRCC survival

Considering the great impact of *MIOX* in ccRCC, we further investigated the association between *MIOX* and ccRCC clinical features and survival evaluation based on TCGA data. ROC analysis showed that *MIOX* could distinguish ccRCC samples from normal samples (Fig. 2A, AUC 0.667), suggesting its potential diagnostic value in the clinical setting. Survival analysis suggested that *MIOX* expression was linked to ccRCC overall survival (Fig. 2B, $P < 0.001$), disease specifical survival (Fig. 2C, $P < 0.001$), and progression-free interval (Fig. 2D, $P < 0.001$). Consistent with this, KM plotter database investigations showed a similar result (Fig. 2E, $P < 0.0001$). In addition, *MIOX* expression was decreased in advanced ccRCC (Fig. 2F, $P < 0.01$). Regarding the TNM stage, *MIOX* exhibited high expression levels in the M0 and stage I (Fig. 2G and H, $P < 0.01$). These results indicated that *MIOX* was engaged in ccRCC early progression. Notably, among ccRCC samples, *MIOX* was enhanced in ccRCC OS survivors, DSS survivors, and PFI survivors (Fig. 2I-K, $P < 0.001$). Collectively, the findings implied that *MIOX* could be considered a favorable prognostic indicator. Furthermore, we also validated that MIOX is lowly expressed in ccRCC tissue sections in The Human Protein Atlas (HPA) database (Supplementary Figure 1A).

miR-4537 is up-regulated in ccRCC and associated with ferroptosis

To further explore the role of miR-4537 in ccRCC, we first investigated the correlation between MIOX expression and miR-4537. Using data from the TargetScan database, we predicted potential miRNAs that could target MIOX. Among the up-regulated miRNAs in ccRCC, we identified four common candidates: miR-4537, miR-4635, miR-4538,

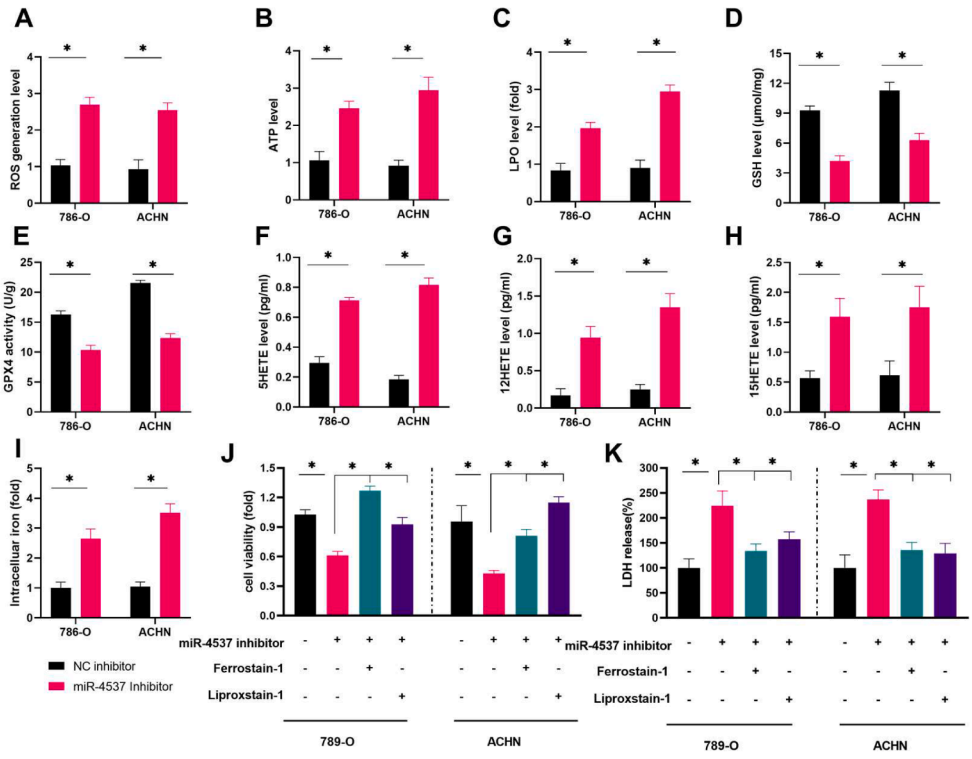

Fig. 5. miR-4537 inhibitor contributed to oxidative Stresstive stress and iron metabolism in ccRCC. (A-C) ROS, ATP, and LPO generation in cells transfected with miR-4537 inhibitor. (D-E) The activity of GSH and GPX4 in cells treated with miR-4537 inhibitors. (F-H) The release of 5-HETE, 12-HETE, and 15-HETE from treated cells. (I) Relative iron level in ccRCC cells stimulated with miR-4537 inhibitor. (J-K) Cell viability and LDH leak in 786-O and ACHN cells co-transfected with miR-4537 inhibitor and Ferrostain-1 or Liproxstain-1. (ns, not significant; *$P < 0.05$).

and miR-8083 (Fig. 3A). The list of related miRNAs has been placed in Supplementary File 1. Notably, miR-4537 was significantly upregulated in ccRCC cell lines when compared to proximal tubule cell lines (Fig. 3B, $P < 0.01$), while the other three miRNAs showed insignificant expression as compared to proximal tubule cell lines (Fig. 3C-E). To illustrate the complex connection between miR-4735 and ferroptosis, we exposed the ccRCC cell lines to well-known ferroptosis triggers, Erastin or RSL3 with DMSO as a negative control [26]. Results showed that either Erastin or RSL3 strongly impeded miR-4537 expression in ccRCC cells (Fig. 3F and G, $P < 0.05$). These findings revealed a potential tie between miR-4537 and ferroptosis in ccRCC. To enrich the research, we present some relevant information about MIOX and miR-4537 in Supplementary Figure 1B, C.

Reduced proliferation of ccRCC cells in colony formation assay following miR-4537 inhibition

To uncover the effect of miR-4537 on ccRCC cells, both a miR-4537 inhibitor and negative control were utilized. The miR-4537 inhibitor successfully reduced miR-4537 levels in ccRCC cell lines (Fig. 4A, $P < 0.05$). Furthermore, suppression of miR-4537 expression significantly impaired the colony-forming capability of both cell lines (Fig. 4B, $P < 0.05$). CCK-8 assay showed that ccRCC cells treated with miR-4537 inhibitor abated cell proliferation rate (Fig. 4C and D, $P < 0.05$). Alternatively, we examined the cell viability and noted that miR-4537 inhibitor stimulation could intensify LDH abundance in ccRCC cells (Fig. 4E, $P < 0.05$), meaning that miR-4537 was an unfavorable factor in tumor cell survival.

miR-4537 inhibitor increased oxidative stress and iron metabolism of ferroptosis in ccRCC

We collaborated to ascertain if blocking miR-4537 could stifle ferroptosis in ccRCC cells, given the known relation between miR-4537 and ferroptosis. Notably, there was a notable rise in the generation of ROS within miR-4537 inhibitor reagent transfected cells (Fig. 5A, $P < 0.05$). Reducing miR-4537 expression led to the decrease of ATP in both 786-O and ACHN cells (Fig. 5B, $P < 0.05$). As previously described, LPO was identified as a crucial marker in ferroptosis. Our results indicated that the LPO level was significantly increased once cells were treated with miR-4537 inhibitor (Fig. 5C, $P < 0.05$). These two key factors were also examined. Results demonstrated that miR-4537 inhibitor fillip trimmed GSH and GPX4 activity in two ccRCC cell lines (Fig. 5D and 5E, $P < 0.05$). It also confirmed that polyunsaturated fatty acids (PUFAs) were oxidized into HETEs when explored in overwhelming ROS signal [27]. In this study, levels of 5-HETE, 12-HETE, and 15-HETE were elevated in cells that had been transfected with an inhibitor of miR-4537 (Fig. 5F-H, $P < 0.05$). Iron enriched in the oxygen context produced ROS by oxidizing phospholipid and fatty acid hydroperoxides [28]. Following the administration of the miR-4537 inhibitor, iron was significantly accumulated in ccRCC cell lines relative to the controls (Fig. 5I, $P < 0.05$). To delineate the contribution of ferroptosis to the observed anti-tumor effects mediated by inhibition of miR-4537, treatments with ferrostatin-1 or liproxstatin-1, established ferroptosis blockers, were subsequently applied to these cell lines. The suppressive cell viability and excessive LDH generation triggered by miR-4537 inhibitor could be reversed by ferrostain-1 or liproxstatin-1 (Fig. 5J and K, $P < 0.05$).

miR-4537 mimic drives ccRCC cell proliferation via cck-8 asssay

786-O cells and ACHN cells were stimulated with a miR-4537 mimic to investigate the role of miR-4537 in ccRCC through a gain-of-function experiment. The miR-4537 imitator increased the levels of endogenous miRNA in ccRCC cells (Fig. 6A, $P < 0.05$). Results showed that enhancing miR-4537 expression increased cell growth rate, suggesting

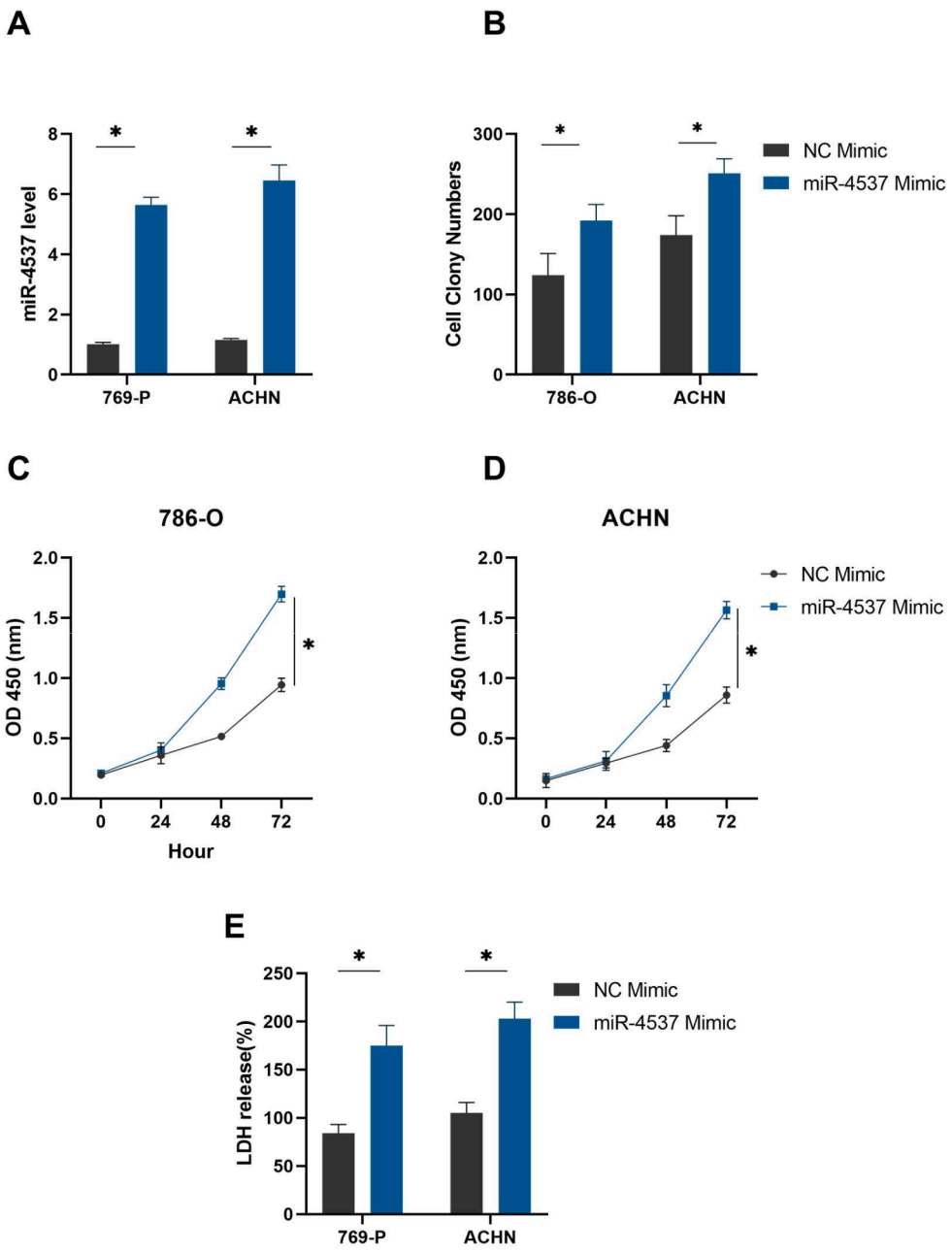

Fig. 6. miR-4537 mimic promotes cell growth. (A) miR-4537 mimic enhanced miR-4537 expression in ccRCC cells. (B) miR-4537 mimic increased cell colony production capability. (C-D) miR-4537 mimic boosted cell proliferation compared with negative control. (E) miR-4537 mimic accelerated LDH generation in ccRCC cells. (ns, not significant; *$P < 0.05$).

that cell viability was also improved (Fig. 6B, $P < 0.05$). CCK-8 data illustrated the cells treated with miR-4537 mimic displayed a higher proliferation pace than cells treated with negative control mimic (Fig. 6C and D, $P < 0.05$). In addition, we measured the live cell amounts after accepting the miR-4537 mimic stimulus. Data showed that miR-4537 was a favorable factor in the call survival environment (Fig. 6E, $P < 0.05$). Taken together, we concluded that miR-4537 was an active contributor to aggravating ccRCC advancement.

miR-4537 mimic hampers antioxidant status and iron metabolism of ferroptosis process in ccRCC

We also explored the association between miR-4537 mimic and ferroptosis. ROS and ATP generation in cells were significantly reduced in the miR-4537 overload environment (Fig. 7A and B, $P < 0.05$). In line with this, intracellular LPO volume was decreased (Fig. 7C, $P < 0.05$). GSH and GPX4 activities exhibited an elevation (Fig. 7D and E, $P < 0.05$). Moreover, the output of HETEs dependent on PUFA in the ROS context was also tested. Results manifested that cells exposed to high miR-4537 expression decreased 5-HETE, 12HETE, and 15HETE generation (Fig. 7F-H, $P < 0.05$), which were caused by LPO in ferroptosis. Most importantly, miR-4537 mimic relived iron load, reducing the iron accumulation in the cell (Fig. 7I, $P < 0.05$). Intriguingly, our rescue assay observed that either ferrostain-1 or liproxstatin-1 alleviated the acceleration of cell viability (Fig. 7J). Of course, the receding LDH level caused by the miR-4537 mimic was also blocked by ferroptosis inducer ferrostain-1 or liproxstatin-1 (Fig. 7K, $P < 0.05$).

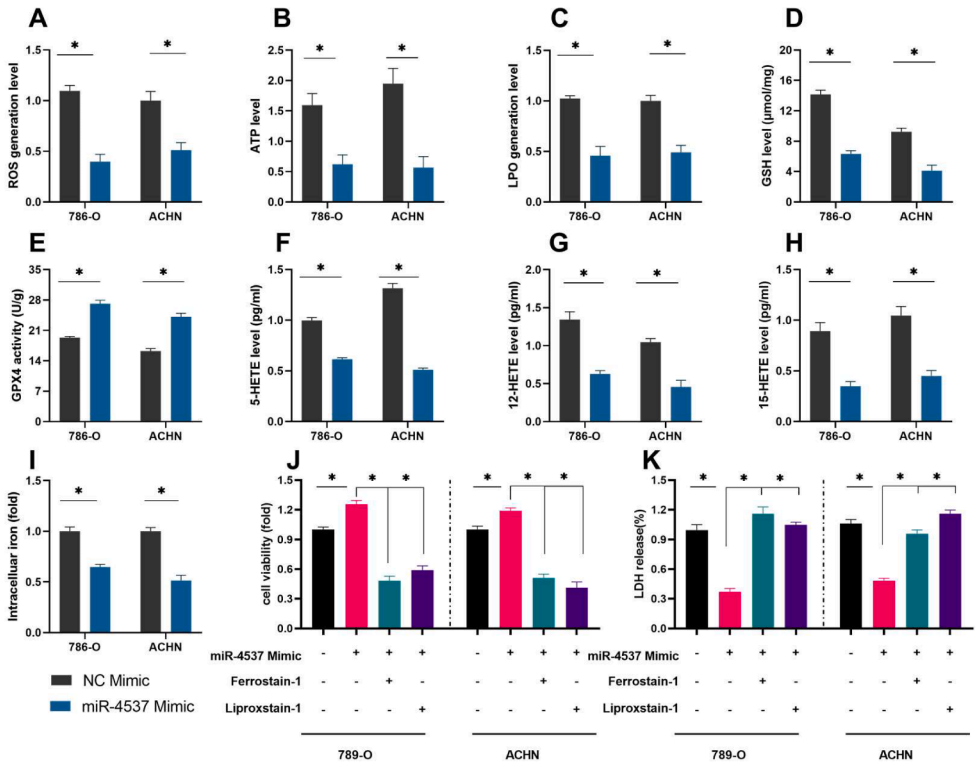

Fig. 7. miR-4537 mimic inhibited cell ferroptosis in ccRCC. (A-C) ROS, ATP, and LPO leak in cells transfected with miR-4537 mimic. (D-E) GSH and GPX4 activity in cells treated with miR-4537 mimic. (F-H) The levels of 5-HETE,12-HETE, and 15-HETE in cell media transfected with miR-4537 mimic. (I) The level of relative iron in ccRCC cells stimulated with miR-4537 mimic. (J-K) Cell viability and LDH leak in 786-O cells and ACHN cells co-transfected with miR-4537 mimic and Ferrostain-1 or Liproxstain-1. (ns, not significant; *$P < 0.05$).

Luciferase reporter assay revealed the binding between miR-4537 and MIOX

Based on our findings, we sought to deepen the regulatory interaction between miR-4537 and *MIOX* in the context of ferroptosis within ccRCC. Initial analysis utilizing the Targetscan database identified a potential miR-4537 target within the 3′-UTR of *MIOX* (Fig. 8A). Luciferase reporter experiment confirmed that miR-4537 directly recognized 3′-UTR of *MIOX* (Fig. 8B, $P < 0.05$). Moreover, transfection with a miR-4537 inhibitor resulted in an upregulation of *MIOX* expression (Fig. 8C and D, $P < 0.05$). Conversely, introduction of a miR-4537 mimic led to diminished *MIOX* expression in ccRCC cell lines (Fig. 8D and E, $P < 0.05$). This research indicated that miR-4537 negatively regulated *MIOX* to impair ferroptosis in ccRCC. In summary, we discovered that in ccRCC, miR-4537 was directly recognized with the *MIOX*, which inhibited ferroptosis. Suppressing miR-4537 could be a novel alternative strategy in ccRCC therapy (Fig. 9).

Discussion

It has been documented that patients suffering from metastatic ccRCC survive less than 10 % of their five years once diagnosed despite it being identified as a curable disease [29]. Although current anti-cancer therapy such as novel immunotherapy has been applied in a clinical trial, the outcomes are not expected as encouraging because of insensitive to immune checkpoint blockade therapy [30]. Recently, ferroptosis, emerging as a hotpot in cancer treatment, has been riddled with challenges. Increasing ferroptosis-associated genes have been identified. Ferroptosis-associated genes, also known as ferroptosis regulators, can be categorized into different gene sets based on their roles: drivers, suppressors, markers, unclassified regulators, inducers, inhibitors, and ferroptosis-disease associations. A prominent characteristic of ferroptosis is the substantial increase in lipid peroxides., which is established as the crux of ferroptosis. Indeed, according to recent findings, the animosity between ferroptosis driving systems and ferroptosis defending executors leads to exceeding LPO in the cell membranes [31–33]. Generally, when ferroptosis-defending families such as the GPX4-GSH signal axis existing in cytoplasm and mitochondria fail to remission the overwhelming ferroptosis-driving activities such as PUFA-PL synthesis, iron, and mitochondrial metabolism, ferroptosis occurs. Distinct from other regulated cell death implemented by a series of executioner proteins such as apoptosis triggered by caspase proteins, cells undergoing ferroptosis have a unique oxidized phospholipid portrait [34].

In the field of cancer treatment, significant advancements have been made in comprehending the significance of ferroptosis. For one thing, well-known tumor suppressors including P53 and BAP1 have been reported to serve a functional purpose in ferroptosis, which demonstrated that ferroptosis serves as a natural obstacle in tumorigenesis [35,36]. For another thing, the engagement of an oncogene or oncogene-associated signaling network in ferroptosis also entitles ferroptosis to an oncogenic role in cancer development [37]. However, the research concerning the association between ferroptosis and ccRCC is very limited. This research concentrated on gene sets that drive ferroptosis and aimed to target the down-regulated mRNA in the TCGA ccRCC cohort, thus elucidating the link between ferroptosis and ccRCC progression. Among nine identified genes, *MIOX* was uniquely found to be crippled in ccRCC cells ($P < 0.05$). Elevated *MIOX* levels yielded augmented ROS generation and decreased nicotinamide adenine dinucleotide phosphate abundance, rendering cell membranes more vulnerable to oxidative damage [38]. Furthermore, we explored the relationship between *MIOX* levels and patient survival outcomes in ccRCC. MIOX expression was significantly associated with overall survival, disease-specific survival, and progression-free survival ($P < 0.001$), indicating that higher *MIOX* levels hinted at a favorable prognosis outcome. Notably, *MIOX* expression was higher in the OS, DSS, and PFS survivor groups than in non-survivor groups, which further

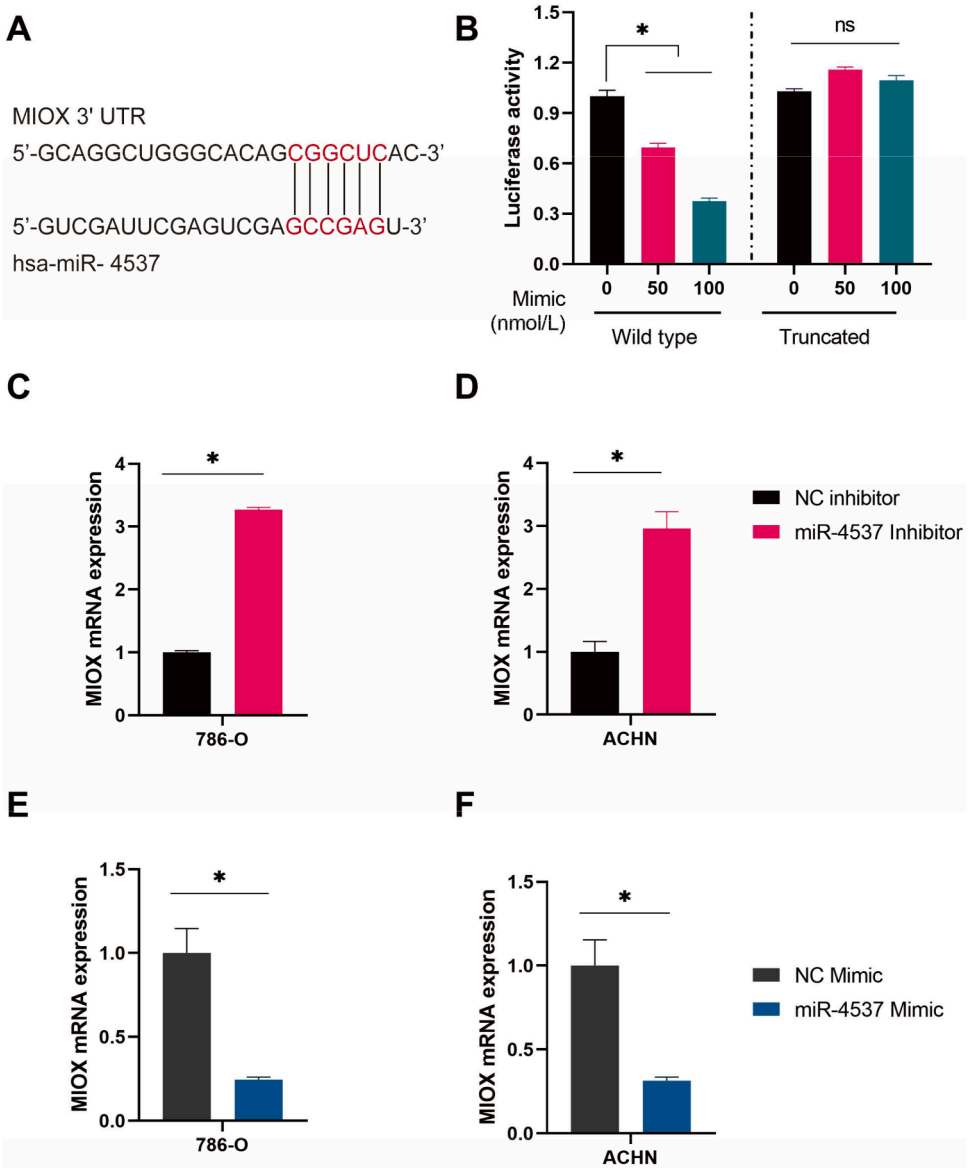

Fig. 8. miR-4537 controlled MIOX expression in ccRCC. (A)The binding sites between miR-4537 and MIOX. (B) The relative luciferase activity. (C-D) miR-4537 inhibitor enhanced MIOX expression in 786-O cells and ACHN cells. (E-F) miR-4537 mimic reduced MIOX expression in 786-O and ACHN cells. (ns, not significant; *$P < 0.05$).

emphasized the great impact of *MIOX* in ccRCC survival ($P < 0.05$). Indeed, *MIOX* was reduced in advanced ccRCC status and advanced TNM stage ($P < 0.05$). Collectively, our findings demonstrate that MIOX functions as a suppressor of tumor growth in ccRCC. Of course, more research will be needed to certify this.

It has been widely accepted that miRNA directly binds with 3′-UTR of target mRNA to exert a far-reaching influence on multiple human cancers. Here, we predicted the potential miRNAs interacting with *MIOX* and obtained the up-regulated miRNA from the TCGA ccRCC dataset. By taking the intersection, 4 miRNAs were discovered. Among these, miR-4537 was highly expressed in ccRCC cells ($P < 0.05$). Nevertheless, its role and exact regulatory mechanisms in ccRCC remain unclear. Not much is known about the relationship of miRNA and ferroptosis in cancer. Here, we investigated the role of miR-4537 in ccRCC. We found that miR-4537 was significantly upregulated in 786-O cells and ACHN cells ($P < 0.05$). Reduced cell proliferation was observed when miR-4537 expression was inhibited, while the reverse effect was seen with miR-4537 overexpression. These studies suggest that miR-4537 serves a purpose in ccRCC development by regulating cell growth through gain and loss-of-function experiments. An isolated study found that miR-4537 could restrict cell proliferation while promoting apoptosis and improving the radiosensitivity of gastric cancer [39]. It is conclusive that the role of miR-4537 depends on the cancer context.

Functional enhancement and suppression experiments were conducted to dissect the role of miR-4537 in ferroptosis in ccRCC. Results demonstrated that miR-4537 expression was greatly decreased once ferroptosis inducer treatment ($P < 0.05$). miR-4537 inhibitor ebbed cell proliferation by governing the ferroptosis process while miR-4537 mimic produced the opposed effects in ccRCC cell lines. miR-4537 inhibitor aggravated intercellular iron load, causing excessive ROS generation, which was a crucial signal in ferroptosis. An overabundance of ROS triggered a series of oxidative stress events, resulting in the peroxidation of PUFAs and lipids. The high levels of LPO were also backed up by the enhanced synthesis of 5-HETE, 12-HETE, and 15-HETE in ccRCC cell lines ($P < 0.05$). Moreover, our luciferase-reporter assay confirmed that miR-4537 could directly perceive the binding sites of MIOX as expected and slashed MIOX transcript abundance. Similarly, the miR-4537 inhibitor urged MIOX expression ($P < 0.05$). MIOX

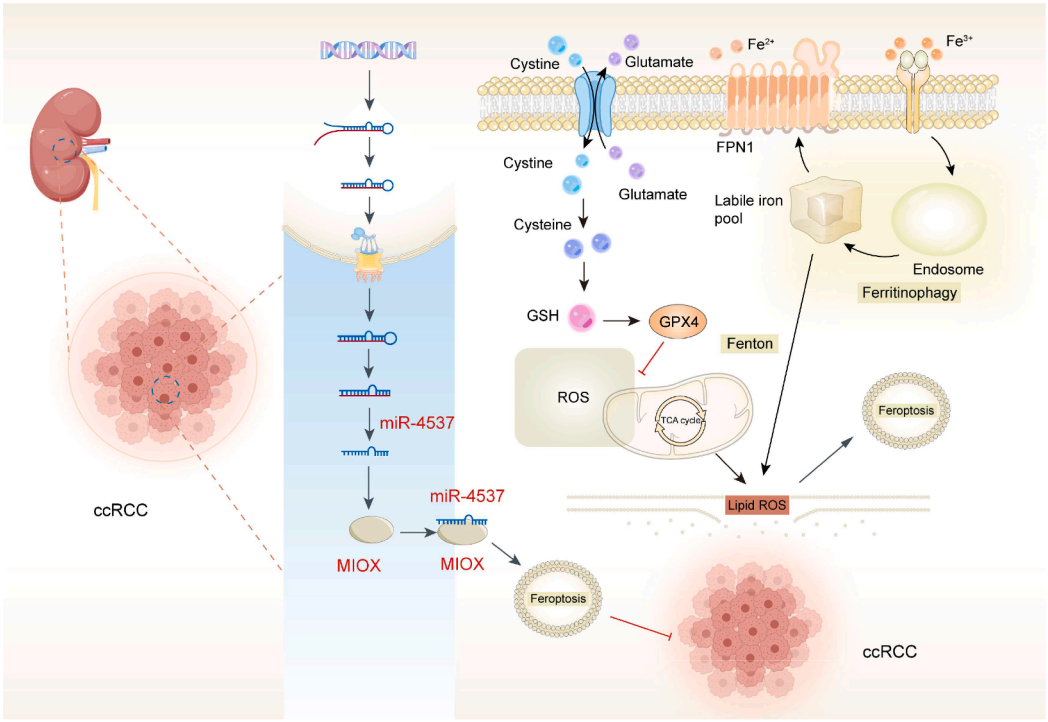

Fig. 9. miR-4537 curtails ferroptosis by targeting *MIOX* in ccRCC.

denotes a proximal tubular enzyme responsible for the transformation of inositol to d-glucuronide via the glucuronide pathway [40]. MIOX has been reported to exacerbate cellular redox injury through expediting ferroptosis in the context of cisplatin induction. Oxidative stress, elevated glucose, and free fatty acids influence MIOX transcription [41]. Increased MIOX expression could amplify ferroptosis through the promotion of ferritinophagy and LPO. Additionally, it could disrupt the ferroptosis inhibition pathway by diminishing GPX4 activities and GSH concentrations within cells [42]. Highly enriched amplification of MIOX reinforces ferroptosis-mediated cell damage, while MIOX downregulation ameliorates this perturbation. In general, we proved that miR-4537 was highly expressed and prohibits ferroptosis by interacting with MIOX in ccRCC. Nonetheless, our study's scope is tempered by inherent limitations. Primarily unfolded in vitro using select ccRCC cell lines, the translatability of these results to in vivo contexts and their generalizability across a wider spectrum of ccRCC variants stand on uncertain ground. Additionally, our reliance on the TCGA ccRCC database and Ferrdb to dissect essential regulatory players indicates that delving deeper into the network of ferroptosis-related genes and pathways may not only unveil more profound insights but also chart new territories in therapeutic discovery.

Conclusion

In this study, we demonstrate that miR-4537 plays a pivotal role in regulating ferroptosis in ccRCC by targeting MIOX. Our findings suggest that miR-4537 exerts its influence on ferroptosis by modulating the expression of MIOX, a key enzyme involved in the oxidative stress response. By targeting MIOX, miR-4537 not only influences cellular iron metabolism but also contributes to the overall redox balance, which is essential for maintaining cancer cell viability. Importantly, these findings highlight the therapeutic potential of targeting miR-4537 to modulate ferroptosis in ccRCC. This study lays the foundation for future research into miRNA-based therapies and opens new avenues for the clinical management of ccRCC, with the promise of improving treatment outcomes for patients with this challenging malignancy

Availability of data and materials

The dataset supporting the conclusions of this article is included within the article.

Funding

None.

Supplementary Figure 1. Correlation analysis of MIOX and miR-4537 (A) Expression of MIOX in human tissue sections (B) Correlation between MIOX and miR-4537 (C) Pathway enrichment analysis of miR-4537

CRediT authorship contribution statement

Hui Li: Writing – review & editing, Writing – original draft, Visualization, Validation, Supervision, Software, Resources, Project administration, Methodology, Investigation, Formal analysis, Data curation, Conceptualization. **Mengyu Fu:** Writing – review & editing, Writing – original draft, Formal analysis, Data curation, Conceptualization. **Lingli Wang:** Writing – review & editing, Writing – original draft, Data curation. **Yanpeng Dai:** Writing – review & editing, Writing – original draft. **Zongxing Lv:** Writing – review & editing, Writing – original draft. **Shilin Geng:** Writing – review & editing.

Declaration of competing interest

The authors declare that they have no competing interests.

Acknowledgements

None.

Supplementary materials

Supplementary material associated with this article can be found, in the online version, at doi:10.1016/j.tranon.2025.102401.

Reference

[1] B. Ljungberg, L. Albiges, Y. Abu-Ghanem, K. Bensalah, S. Dabestani, S. Fernández-Pello, R.H. Giles, F. Hofmann, M. Hora, M.A. Kuczyk, et al., European association of urology guidelines on renal cell carcinoma: the 2019 update, Eur. Urol. 75 (5) (2019) 799–810.

[2] L. Shan, W. Liu, Y. Zhan, Long Non-coding RNA CCAT1 acts as an oncogene and promotes sunitinib resistance in renal cell carcinoma, Front. Oncol. 10 (2020) 516552.

[3] E. Jonasch, J. Gao, W.K. Rathmell, Renal cell carcinoma, BMJ 349 (2014) g4797.

[4] E. Jonasch, C.L. Walker, W.K. Rathmell, Clear cell renal cell carcinoma ontogeny and mechanisms of lethality, Nat. Rev. Nephrol. 17 (4) (2021) 245–261.

[5] D.C. Yang, C.-H. Chen, Potential New Therapeutic Approaches for Renal Cell Carcinoma, Semin. Nephrol. 40 (1) (2020) 86–97.

[6] X. Chen, R. Kang, G. Kroemer, D. Tang, Broadening horizons: the role of ferroptosis in cancer, Nat. Rev. Clin. Oncol. 18 (5) (2021) 280–296.

[7] B. Hassannia, P. Vandenabeele, T. Vanden Berghe, Targeting Ferroptosis to Iron Out Cancer, Cancer Cell 35 (6) (2019) 830–849.

[8] M. Conrad, S.M. Lorenz, B. Proneth, Targeting ferroptosis: new hope for as-yet-incurable diseases, Trends. Mol. Med. 27 (2) (2021) 113–122.

[9] S.J. Dixon, K.M. Lemberg, M.R. Lamprecht, R. Skouta, E.M. Zaitsev, C.E. Gleason, D.N. Patel, A.J. Bauer, A.M. Cantley, W.S. Yang, et al., ferroptosis: an iron-dependent form of nonapoptotic cell death, Cell 149 (5) (2012) 1060–1072.

[10] Z. Chen, W. Wang, S.R. Abdul Razak, T. Han, N.H. Ahmad, X. Li, Ferroptosis as a potential target for cancer therapy, Cell Death. Dis. 14 (7) (2023) 460.

[11] G. Lei, L. Zhuang, B. Gan, **Targeting ferroptosis as a vulnerability in cancer**, Nat. Rev. Cancer 22 (7) (2022) 381–396.

[12] E. Dai, L. Han, J. Liu, Y. Xie, H.J. Zeh, R. Kang, L. Bai, D. Tang, Ferroptotic damage promotes pancreatic tumorigenesis through a TMEM173/STING-dependent DNA sensor pathway, Nat. Commun. 11 (1) (2020) 6339.

[13] V.E. Kagan, G. Mao, F. Qu, J.P.F. Angeli, S. Doll, C.S. Croix, H.H. Dar, B. Liu, V. A. Tyurin, V.B. Ritov, et al., **Oxidized arachidonic and adrenic PEs navigate cells to ferroptosis**, Nat. Chem. Biol. 13 (1) (2017) 81–90.

[14] D.P. Bartel, MicroRNAs: genomics, biogenesis, mechanism, and function, Cell 116 (2) (2004) 281–297.

[15] P. Popławski, J. Bogusławska, K. Hanusek, A. Piekiełko-Witkowska, Nucleolar proteins and non-coding RNAs: roles in renal Cancer, Int. J. Mol. Sci. 22 (23) (2021).

[16] R. Yousefpour Shahrivar, F. Karami, E. Karami, Differential gene expression patterns in Niemann-Pick Type C and Tay-Sachs diseases: implications for neurodegenerative mechanisms, PLoS One 20 (3) (2025) e0319401.

[17] Y. Cao, J. Li, Y. Chen, Y. Wang, Z. Liu, L. Huang, B. Liu, Y. Feng, S. Yao, L. Zhou, et al., Monounsaturated fatty acids promote cancer radioresistance by inhibiting ferroptosis through ACSL3, Cell Death. Dis. 16 (1) (2025) 184.

[18] Y. Zhu, L. Yang, J. Xu, X. Yang, P. Luan, Q. Cui, P. Zhang, F. Wang, R. Li, X. Ding, et al., Discovery of the anti-angiogenesis effect of eltrombopag in breast cancer through targeting of HuR protein, Acta Pharm. Sin. B 10 (8) (2020) 1414–1425.

[19] Z. Sun, Y. Wang, C. Zheng, L. Xiao, Y. Zang, L. Fang, X. Cui, M. Chang, Q. Sun, W. Li, et al., NAT10 promotes the progression of clear cell renal cell carcinoma by regulating ac4C acetylation of NFE2L3 and activating AKT/GSK3β signaling pathway, Cell Death. Dis. 16 (1) (2025) 235.

[20] M. Brodmann, R.F. Dreier, P. Broz, M. Basler, Francisella requires dynamic type VI secretion system and ClpB to deliver effectors for phagosomal escape, Nat. Commun. 8 (2017) 15853.

[21] J. Yu, J. Deng, L. Ren, L. Hua, T. Wu, Y. Hui, C. Shao, Y. Gong, A high content clonogenic survival drug screening identifies maytansine as a potent radiosensitizer for meningiomas, Front. Immunol. 16 (2025) 1557165.

[22] W.S. Yang, R. SriRamaratnam, M.E. Welsch, K. Shimada, R. Skouta, V. S. Viswanathan, J.H. Cheah, P.A. Clemons, A.F. Shamji, C.B. Clish, et al., Regulation of ferroptotic cancer cell death by GPX4, Cell 156 (1–2) (2014) 317–331.

[23] S. Okazaki, K. Umene, J. Yamasaki, K. Suina, Y. Otsuki, M. Yoshikawa, Y. Minami, T. Masuko, S. Kawaguchi, H. Nakayama, et al., Glutaminolysis-related genes determine sensitivity to xCT-targeted therapy in head and neck squamous cell carcinoma, Cancer Sci. 110 (11) (2019) 3453–3463.

[24] J. Lee, J.H. You, D. Shin, J.-L. Roh, Inhibition of Glutaredoxin 5 predisposes Cisplatin-resistant Head and Neck Cancer Cells to Ferroptosis, Theranostics 10 (17) (2020) 7775–7786.

[25] Y. Pan, Z. Xie, S. Cen, M. Li, W. Liu, Tang Sa, G. Ye, J. Li, G. Zheng, Z. Li, et al., Long noncoding RNA repressor of adipogenesis negatively regulates the adipogenic differentiation of mesenchymal stem cells through the hnRNP A1-PTX3-ERK axis, Clin. Transl. Med. 10 (7) (2020) e227.

[26] Z.H. Lin, Y. Liu, N.J. Xue, R. Zheng, Y.Q. Yan, Z.X. Wang, Y.L. Li, C.Z. Ying, Z. Song, J. Tian, et al., Quercetin Protects against MPP(+)/MPTP-Induced Dopaminergic Neuron Death in Parkinson's Disease by Inhibiting Ferroptosis, Oxid. Med. Cell Longev. 2022 (2022) 7769355.

[27] Z. Tang, W. Jiang, M. Mao, J. Zhao, J. Chen, N. Cheng, Deubiquitinase USP35 modulates ferroptosis in lung cancer via targeting ferroportin, Clin. Transl. Med. 11 (4) (2021) e390.

[28] U. Barayeu, D. Schilling, M. Eid, T.N. Xavier da Silva, L. Schlicker, N. Mitreska, C. Zapp, F. Gräter, A.K. Miller, R. Kappl, et al., Hydropersulfides inhibit lipid peroxidation and ferroptosis by scavenging radicals, Nat. Chem. Biol. (2022).

[29] L. Dell'Atti, N. Bianchi, G. Aguiari, New therapeutic interventions for kidney carcinoma: looking to the future, Cancers 14 (15) (2022).

[30] K. Zheng, L. Gao, J. Hao, X. Zou, X. Hu, An immunotherapy response prediction model derived from proliferative CD4 T cells and antigen-presenting monocytes in ccRCC, Front. Immunol. 13 (2022) 972227.

[31] C. Mao, X. Liu, Y. Zhang, G. Lei, Y. Yan, H. Lee, P. Koppula, S. Wu, L. Zhuang, B. Fang, et al., DHODH-mediated ferroptosis defence is a targetable vulnerability in cancer, Nature 593 (7860) (2021) 586–590.

[32] V.A.N. Kraft, C.T. Bezjian, S. Pfeiffer, L. Ringelstetter, C. Müller, F. Zandkarimi, J. Merl-Pham, X. Bao, N. Anastasov, J. Kössl, et al., GTP cyclohydrolase 1/tetrahydrobiopterin counteract ferroptosis through lipid remodeling, ACS Cent. Sci. 6 (1) (2020) 41–53.

[33] K. Bersuker, J.M. Hendricks, Z. Li, L. Magtanong, B. Ford, P.H. Tang, M.A. Roberts, B. Tong, T.J. Maimone, R. Zoncu, et al., The CoQ oxidoreductase FSP1 acts parallel to GPX4 to inhibit ferroptosis, Nature 575 (7784) (2019) 688–692.

[34] B. Wiernicki, H. Dubois, Y.Y. Tyurina, B. Hassannia, H. Bayir, V.E. Kagan, P. Vandenabeele, A. Wullaert, T. Vanden Berghe, Excessive phospholipid peroxidation distinguishes ferroptosis from other cell death modes including pyroptosis, Cell Death. Dis. 11 (10) (2020) 922.

[35] L. Jiang, N. Kon, T. Li, S.J. Wang, T. Su, H. Hibshoosh, R. Baer, W. Gu, Ferroptosis as a p53-mediated activity during tumour suppression, Nature 520 (7545) (2015) 57–62.

[36] Y. Zhang, J. Shi, X. Liu, L. Feng, Z. Gong, P. Koppula, K. Sirohi, X. Li, Y. Wei, H. Lee, et al., BAP1 links metabolic regulation of ferroptosis to tumour suppression, Nat. Cell Biol. 20 (10) (2018) 1181–1192.

[37] J. Yi, J. Zhu, J. Wu, C.B. Thompson, X. Jiang, Oncogenic activation of PI3K-AKT-mTOR signaling suppresses ferroptosis via SREBP-mediated lipogenesis, Proc. Natl. Acad. Sci. USA 117 (49) (2020) 31189–31197.

[38] Y. Kinowaki, M. Kurata, S. Ishibashi, M. Ikeda, A. Tatsuzawa, M. Yamamoto, O. Miura, M. Kitagawa, K. Yamamoto, Glutathione peroxidase 4 overexpression inhibits ROS-induced cell death in diffuse large B-cell lymphoma, Lab. Invest. 98 (5) (2018) 609–619.

[39] J. Liu, S. Yan, J. Hu, D. Ding, Y. Liu, X. Li, H.S. Pan, G. Liu, B. Wu, Y. Liu, MiRNA-4537 functions as a tumor suppressor in gastric cancer and increases the radiosensitivity of gastric cancer cells, Bioengineered 12 (1) (2021) 8457–8467.

[40] R.J. Arner, K.S. Prabhu, C.C. Reddy, Molecular cloning, expression, and characterization of myo-inositol oxygenase from mouse, rat, and human kidney, Biochem. Biophys. Res. Commun. 324 (4) (2004) 1386–1392.

[41] R.K. Dutta, V.K. Kondeti, I. Sharma, N.S. Chandel, S.E. Quaggin, Y.S. Kanwar, Beneficial Effects of -Inositol Oxygenase Deficiency in Cisplatin-Induced AKI, J. Am. Soc. Nephrol. 28 (5) (2017) 1421–1436.

[42] F. Deng, I. Sharma, Y. Dai, M. Yang, Y.S. Kanwar, Myo-inositol oxygenase expression profile modulates pathogenic ferroptosis in the renal proximal tubule, J. Clin. Invest. 129 (11) (2019) 5033–5049.